

All-optical clock recovery for 40 Gbaud NRZ-QPSK signals using amplified feedback DFB laser diode

Liqliang Yu (余力强)¹, Yan Li (李岩)², Jizhao Zang (臧继召)², Dan Lu (陆丹)^{1*},
Biwei Pan (潘碧玮)¹, and Lingjuan Zhao (赵玲娟)¹

¹Key Laboratory of Semiconductor Materials Science, Institute of Semiconductors,
Chinese Academy of Sciences, Beijing 100086, China

²State Key Laboratory of Information Photonics and Optical Communications, Beijing University
of Posts and Telecommunications, Beijing 100876, China

*Corresponding author: ludan@semi.ac.cn

Received March 1, 2014; accepted April 29, 2014; posted online July 18, 2014

An all-optical clock recovery scheme based on monolithic amplified feedback DFB laser (AFL) diode is proposed for nonreturn-to-zero (NRZ) quadrature phase shift keying (QPSK) format signals. By using a preprocessing stage, clock recovery (CR) is successfully demonstrated for 40-Gbaud NRZ-QPSK signals based on this scheme. The dependence of the timing jitter of the recovered clock on the optical power of the injected signal is investigated. A minimum timing jitter of 362.8 fs (integrated within a frequency range from 10 Hz to 10 MHz) is obtained.

OCIS codes: 140.3520, 230.1150.

doi: 10.3788/COL201412.081402.

In spite of the current dominance of coherent optical transmission using electronic digital signal processing^[1], the need for clock recovery (CR) is still high in all-optical network^[2]. All-optical CR is regarded as a crucial technique for optical signal processing applications, such as 3R regeneration, optical time-division demultiplexing, and modulation format conversion^[3]. Among the various techniques for all-optical CR, schemes based on the amplified feedback DFB laser (AFL) are capable of operating at a high bit rate with simple setup, low power consumption, and compact size^[4–9]. As one kind of monolithic dual-mode semiconductor lasers (MDMSLs), AFL is more attractive since the beat frequency from AFL exhibits a narrower line-width compared to Fabry-Perot (F-P) lasers^[10] or distributed Bragg reflector (DBR) lasers^[11]. Furthermore, when we use MDMSL as the CR device, coherent injection locking^[12] can be easily utilized. Compared to incoherent injection, the coherent injection locking requires lower injection power and its operation speed is not limited by the carrier lifetime^[13].

All-optical CR based on AFL has been demonstrated experimentally at 40 Gb/s^[8]. However, previous works mostly focused on conventional on-off-keying (OOK) modulation formats. Recently, phase modulation formats acquired increasing popularity due to their higher resilience to non-linear impairment and better optical signal to noise ratio sensitivity with respect to usual OOK formats^[14]. All-optical CR approaches used in OOK modulation format can also be applied to return-to-zero differential phase-shift keying (RZ-DPSK) format due to the relative strong clock component in the modulated spectrum^[15]. But, compared to RZ-phase shift keying (PSK) format, it is more difficult to extract a clock signal from a nonreturn-to-zero (NRZ)-PSK signal. In 2008, an all-optical CR directly for NRZ-DPSK signal using a self-pulsating DBR laser was demonstrated^[11],

where the recovered clock had a timing jitter of 760 fs. Furthermore, it was reported that a preprocessing stage was always used to enhance the weak clock so as to extract the clock signal with the all-optical CR technique used for OOK formats. For example, the preprocessing stages of using a DPSK demodulator to convert a NRZ-DPSK signal to a pseudo-RZ (PRZ)-DPSK or RZ-OOK signal were reported in 2006^[16], 2010^[17], and 2012^[18], where the timing jitters of recovered clock signals were 800, 1280, and 575, respectively.

With the development of 100- and 400-G technology, quadrature phase shift keying (QPSK) has become the primary modulation format in optical communication systems. Will the all-optical CR scheme based on MDMSL be a viable way for QPSK system? There is still no definite answer. In this letter, we demonstrate an AFL-based all-optical CR scheme, which can be used to extract the optical clock from Mach-Zehnder-modulator (MZM)-generated NRZ-QPSK signals at a signal rate of 40 Gbaud. Here, with a preprocessing stage consisting of a semiconductor optical amplifier (SOA) as the phase-information-eliminator in the original NRZ-QPSK signal, an enhanced clock tone was obtained in the wavelength-converted signal. We realize the CR and the recovered optical clock signal has a root-mean-square (RMS) timing jitter of 362.8 fs (integrated in the 10 Hz to 10 MHz range). The results indicate that the use of the SOA to eliminate the phase information through wavelength conversion could be extended to higher order modulation formats.

Based on the previous research on the 20-GHz AFL^[9], we design and fabricate an AFL with 40-GHz pulsation frequency. It consists of a gain-coupled DFB section, a phase section and an amplifier section, as shown in Figs. 1(a) and (b). In the AFL, the phase tuning and the

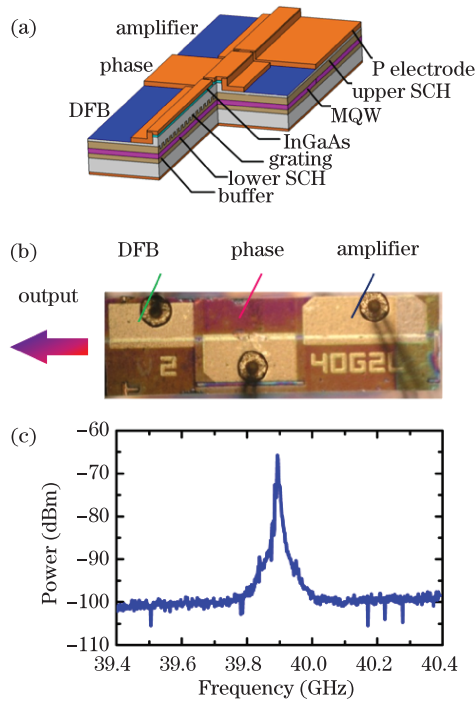


Fig. 1. (Color online) (a) Schematic diagram of the AFL diode. (b) Photograph of the AFL diode. (c) RF spectrum of the free-running AFL diode.

amplifier section act as a feedback cavity and allow the feedback strength and phase to be controlled via injection currents and, accordingly, the pulsation frequency can be tuned. While the DFB section works in a single mode by itself, the optical feedback to the DFB section can give comparable threshold gains to two compound-cavity modes, the beating of which gives rise to pulsation. In the CR process, we inject the signal light into an AFL. When the free-running pulsation is injection locked by the incoming optical signal, the AFL will generate two synchronized modes, whose beating frequency and phase are exactly the same as the incoming clock tone.

A number of AFL devices with various section lengths are measured and showed almost the same behavior for mode-beating self-pulsation. Typical results presented here are obtained from a device with a 220- μm DFB section, a 240- μm phase control section, and a 320- μm amplifier section. In the experiment, the working temperature of the device is controlled at 25 $^{\circ}\text{C}$ by using a thermoelectric cooler (TEC). Here, the currents applied to the DFB section, the phase section, and the amplifier section are 92, 37, and 60 mA, respectively. The laser from the uncoated facet of the DFB section is coupled into a tapered single mode fiber with a coupling efficiency of about 10% and tested by an optical spectrum analyzer (OSA; AQ6370B, Yokogawa, Japan). The wavelength of the AFL is around 1551.6 nm. The self-pulsating frequency is 39.8 GHz and a 3-dB linewidth of 3.2 MHz is observed in the radio (RF) spectrum as shown in Fig. 1(c), where the fiber-coupled-output power of the AFL is -3 dBm.

For MZM-generated NRZ-QPSK signals, the optical power will experience a temporary quick change as a bit changes its phase from one to another. This change in power will yield a weak clock tone in its modulation spec-

trum, which can be used to extract the optical clock. To further improve the clock quality, a preprocessing stage is introduced, where a SOA is used to eliminate the phase information in the incoming QPSK signal through cross gain modulation (XGM) effects, so as to “purify” the clock tone in the incoming signal.

In order to illustrate the operation principle clearly, the setup diagram is divided into three main parts which include the NRZ-QPSK signal generator, the preprocessing stage, and the all-optical CR unit. In this scheme, the QPSK signals are first wavelength-converted to eliminate the phase information by using the SOA. The wavelength-converted signal is then utilized to inject the free-running AFL to realize the clock extraction.

Figure 2 shows the experimental setup of the proposed CR with a preprocessing stage. A transmitter based on MZM driven by a pulse stream was used to generate NRZ-QPSK signals with a carrier wavelength of 1556 nm. The length of the pseudo random bit sequence (PRBS) pattern was 2^7-1 . The coded signal then passed through the EDFA2 and VOA3 to adjust the power of the input signal. The signal was injected into the AFL through an optical circulator and a lensed fiber. An optical band-pass filter (OBPF) with a bandwidth of 0.8 nm was used to eliminate the amplified spontaneous emission (ASE) noise. The amplified recovered clock signal was then analyzed by an optical sampling oscilloscope (OSO) and electrical spectrum analyzer (ESA; E4447A Agilent, USA) through a 50-GHz photo-detector (PD).

Figure 3 shows the measured optical spectrum and eye diagram of the input NRZ-QPSK signal with a carrier wavelength of 1556 nm. The wavelength of the TL2 is

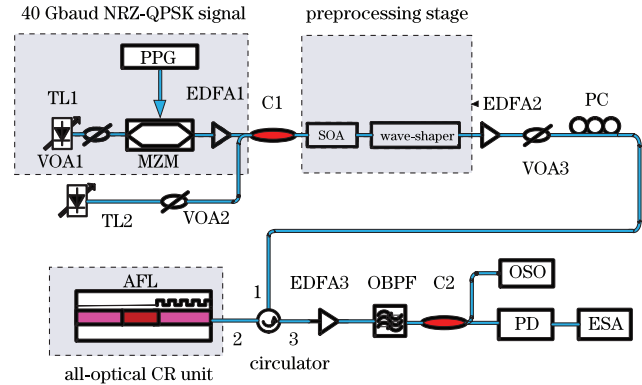


Fig. 2. (Color online) Experimental setup for CR with a preprocessing stage. TL: tunable laser; PPG: pulse pattern generator; VOA: variable optical attenuator; PC: polarization controller; C1&C2: optical coupler.

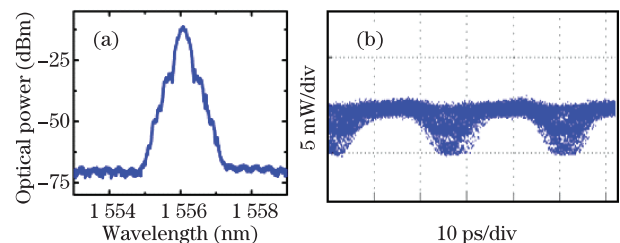


Fig. 3. (Color online) (a) Optical spectrum of the input NRZ-QPSK signal. (b) Eye diagram of the input NRZ-QPSK signal.

tuned to 1551.6 nm. The measured optical spectrum of the signal output from the C1 is shown in Fig. 4(a). After passing through a SOA (SOA-XN-OEC-1550, CIP, China), the phase information of the NRZ-QPSK signal is eliminated and the intensity variation is modulated on the continuous wave (CW) light from TL2 through XGM. As shown in Fig. 4(b), some sidebands arise in the intensity-modulated light from TL2, which gives a clean clock tone. Following the SOA, a wave shaper (WAVESHAPER4000s, Finisar, USA) is used to select the wavelength-converted signal. Then, the signal is set to the same wavelength as that of the free-running AFL so that one of the sidebands is aligned to one mode of the AFL while the signal carrier is aligned to the other mode of the AFL. After the injection of the clock-tone-enhanced signal into the AFL, the lasing optical spectrum exhibits an injection-locked state due to the phase synchronization in the AFL diode, as shown in Fig. 4(c). Finally, a synchronized clock is obtained from the beating of the two injection-locked modes.

To investigate the quality of the recovered clock signal, the trace and the full span RF spectrum of the clock signal are shown in Fig. 5, where the input power is 0 dBm. The input signal power value refers to the power of the optical signal out of the port 2 of the optical circulator, as shown in Fig. 2. The recovered clock shows clear temporal trace at a signal rate of 40 Gbaud, as shown in Fig. 5(a). Figure 5(b) shows that a carrier-to-noise ratio of 36 dB is obtained for the recovered clock, in which both of the resolution bandwidth (RBW) and video bandwidth (VBW) are 910 kHz.

The optical power of the injected signal is adjusted to various levels to evaluate the performance of the recovered clock. Figure 6(a) shows the single sideband (SSB) phase noise of the recovered clock signal where the optical power values are varied from -20 to 6 dBm, in which

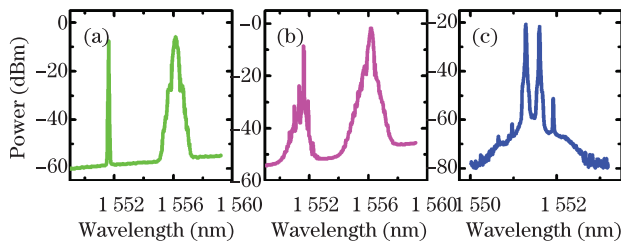


Fig. 4. Optical spectra in the CR setup. (a) After the C1; (b) after the SOA; (c) after injection-locked.

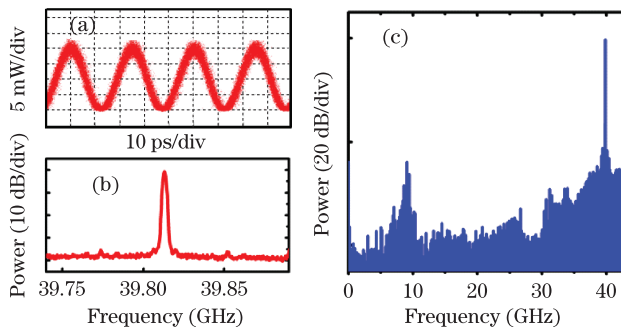


Fig. 5. (Color online) (a) Temporal trace of the recovered clock signal. (b) Detailed RF spectrum of the recovered clock signal. (c) Full span RF spectrum of the recovered clock signal.

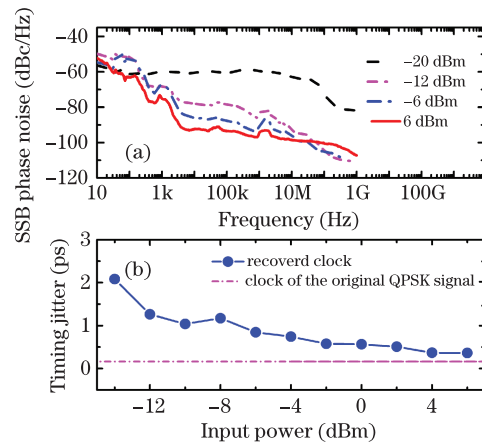


Fig. 6. (Color online) (a) SSB phase noise spectra of the recovered clock signals under various input power values. (b) Dependence of the RMS timing jitter on the optical power of the injected signals.

a significant suppression of the phase noise is obtained by increasing the input power. Figure 6(b) shows the dependence of the RMS timing jitter of the recovered clock on the optical power of the injected signal. As can be seen, when the injected power is less than -4 dBm, the phase noise derived from the AFL diode is suppressed by an increase in the input power. Yet, no further much suppression for the phase noise is obtained when the input power is higher than -4 dBm. The timing jitter changes little when the injected optical power varies from -4 to 6 dBm. When the injected power is 6 dBm, the lowest timing jitter of 362.8 fs is obtained in our experiment, where the timing jitter may be primarily from the input signal. It is worth noting that a timing jitter of 161 fs for the clock of the original QPSK signal corresponds to the jitter noise floor, as shown by the dash line.

In conclusion, we successfully demonstrate all-optical CR for MZM-generated 40-Gbaud NRZ-QPSK signals using a monolithic AFL diode. With a preprocessing stage to enhance the weak clock tone, a low-timing-jitter and robust clock signal is recovered. Through XGM, the SOA being insensitive to phase changes, is used to eliminate the influence from phase information in the original NRZ-QPSK signal and equivalently enhance the clock tones in the wavelength-converted signal. The dependence of the CR on the input signal power is investigated. A minimum timing jitter of 362.8 fs (integrated within a frequency range from 10 Hz to 10 MHz) is obtained in our experiment. As we know, it is the lowest timing jitter for using a quantum-well based laser to extract the clock signal for 40 Gbaud NRZ-QPSK signals.

This work was supported by the National “973” Program of China (No. 2011CB301702), in part by the National “863” Program of China (No. 2013AA014202), and the National Natural Science Foundation of China (Nos. 612011103, 61335009, 61274045, and 61205031).

References

1. Y. Ji, X. Jia, Y. Li, J. Wu, and J. Lin, *Chin. Opt. Lett.* **11**, 050602 (2013).
2. R. Slavík, F. Parmigiani, J. Kakande, C. Lundström, M. Sjödin, P. A. Andrekson, R. Weerasuriya, S. Sygletos, A.

- D. Ellis, L. Grüner-Nielsen, D. Jakobsen, S. Herstrøm, R. Phelan, J. O’Gorman, A. Bogris, D. Syvridis, S. Dasgupta, P. Petropoulos, and D. J. Richardson, *Nature Photon.* **4**, 690 (2010).
3. L. Yin, G. Liu, J. Wu, and J. Lin, *Chin. Opt. Lett.* **4**, 72 (2006).
 4. D. S. Yee, Y. A. Leem, S. B. Kim, D. C. Kim, K. H. Park, S. T. Kim, and B. G. Kim, *Opt. Lett.* **29**, 2243 (2004).
 5. D. S. Yee, Y. A. Leem, S. B. Kim, E. Sim, H. G. Yun, D. C. Kim, and K. H. Park, *IEEE Photon. Technol. Lett.* **17**, 1151 (2005).
 6. Y. Leem, D. Kim, E. Sim, S. Kim, Y. A. Leem, D. C. Kim, E. Sim, S. B. Kim, H. Ko, K. H. Park, D. S. Yee, J. O. Oh, S. H. Lee, and M. Y. Jeon, *IEEE J. Sel. Topics Quantum Electron.* **12**, 726 (2006).
 7. D. Yee, Y. A. Leem, S. T. Kim, K. H. Park, and B.G. Kim, *IEEE J. Quantum Electron.* **43**, 1095 (2007).
 8. C. Chen, Y. Sun, L. Zhao, J. Pan, and J. Qiu, *Opt. Commun.* **284**, 5613 (2011).
 9. Y. Sun, J. Q. Pan, L. J. Zhao, W. X. Chen, W. Wang, L. Wang, X. F. Zhao, and C. Y. Lou, *J. Lightw. Technol.* **28**, 2521 (2010).
 10. F. Wang, Y. Yu, X. Huang, and X. L. Zhang, *IEEE Photon. Technol. Lett.* **21**, 1109 (2009).
 11. X. F. Tang, J. C. Cartledge, A. Shen, F. V. Dijk, and G. H. Duan, *IEEE Photon. Technol. Lett.* **20**, 1443 (2008).
 12. J. F. Qiu, C. Chen, L. J. Zhao, Y. Sun, D. Lu, C. Y. Lou, and W. Wang, *Appl. Opt.* **51**, 2894 (2012).
 13. L. Q. Yu, D. Lu, L. J. Zhao, Y. Li, C. Ji, J. Q. Pan, H. L. Zhu, and W. Wang, *IEEE Photon. Technol. Lett.* **25**, 576 (2013).
 14. X. F. Tang, J. C. Cartledge, A. Shen, A. Akrouf, and G. H. Duan, *Opt. Lett.* **34**, 899 (2009).
 15. X. F. Tang, J. C. Cartledge, A. Shen, F. V. Dijk, A. Akrouf, and G. H. Duan, *J. Lightw. Technol.* **27**, 4603 (2009).
 16. Y. Yu, X. Zhang, and D. Huang, *IEEE Photon. Technol. Lett.* **18**, 2356 (2006).
 17. S. W. Jeon, T. Y. Kim, W. B. Kwon, and C. S. Park, *Opt. Commun.* **283**, 522 (2010).
 18. F. Wang, Y. Yu, Y. Zhang, and X. L. Zhang, *J. Lightw. Technol.* **30**, 1632 (2012).